Polymer Chemistry

RSC Publishing

COMMUNICATION

View Article Online
View Journal | View Issue

Synthesis and photovoltaic properties of novel 3,4-ethylenedithiathiophene-based copolymers for organic solar cells†

Cite this: *Polym. Chem.*, 2013, **4**, 1317

Received 18th November 2012
Accepted 2nd January 2013

DOI: 10.1039/c2py20995k

www.rsc.org/polymers

Xiuxuan Sun,[ab] Weichao Chen,[a] Zhengkun Du,[a] Xichang Bao,[a] Guannan Song,[b] Kangquan Guo,[b] Ning Wang[a] and Renqiang Yang*[a]

Two novel conjugated polymers based on 3,4-ethylenedithiathiophene (EDTT) were designed and synthesized through the palladium-catalyzed Suzuki coupling method and Stille cross-coupling reactions. Conventional and inverted cells were fabricated and device processing conditions were optimized, respectively. The maximum power conversion efficiency (PCE) of 2.4% was obtained with an open-circuit voltage (V_{oc}) of 0.69 V, a short circuit current (J_{sc}) of 6.62 mA cm^{-2}, and a fill factor (FF) of 53%, respectively.

Introduction

Bulk heterojunction polymer solar cells (BHJ-PSCs), which are promising in terms of their potential advantages of low cost,[1,2] light weight,[3] good mechanical flexibility,[4] and simplicity to manufacture,[5,6] have attracted considerable research interest in recent years.[7] BHJ solar cells are prepared from a p (or n)-type organic semiconductor and an electron acceptor (or donor).[8,9] Among a variety of photoactive donor–acceptor composites, the blend of poly(3-hexylthiophene) (P3HT) and [6,6]-phenyl-C_{61}-butyric acid methyl ester (PCBM) has been extensively investigated since cells based on such a composite have a reproducible power conversion efficiency (PCE) of 3–5%.[10] Although the maximum PCE of PSCs increased significantly during the past years,[11,12] which have the potential to compete effectively with alternative solar cell technologies, it is still an urgent issue to explore new types of photovoltaic materials.

It is known that poly(3,4-ethylenedioxythiophene) (PEDOT) was first reported in 1995 by I. Winter *et al.*[13] Since then, numerous variants of EDOT have been investigated,[14] such as 3,4-butylenedioxythiophene (BDOT),[15] thieno[3,4-*b*]-1,4-oxathiane (EOTS),[16] 3,4-ethylenediselenathiophene (EDST),[17] 3,4-ethylenedithiaphosphole (EDPP),[18] *etc.* Moreover, the commercialization of EDOT was begun in 1998 by Bayer AG because of its advantages of high electron conductivity with optical transparency in its oxidized states and high thermal stability. Although there are many reports about the analogues of EDOT, few research associated with 3,4-ethylenedithiathiophene (EDTT) was published. Compared to EDOT, EDTT shows a lower oxidation potential and has a better electronic interaction between polymer chains through intermolecular S–S attractions in its polymeric derivatives.[19] On the other hand, benzodithiophene (BDT) has attracted an increasing amount of attention as a common building block in conjugated polymers and the maximum PCE of BDT-based polymers has improved rapidly.[20,21] For instance, J. Hou *et al.* have synthesized eight new BDT-based polymers with commonly used conjugated units, such as thiophene, benzo[*c*][1,2,5] thiadiazole (BT), thieno[3,4-*b*]pyrazine (TPZ), *etc.*[22] However, there have been no reports on the photovoltaic properties of BDT combining EDTT into one single chain polymer to date. Meanwhile, in order to take advantage of the donor–acceptor (D–A) approach for PSCs, it is proposed that the EDTT unit polymerizes with the electron-deficient isoindigo unit to form copolymers. (*E*)-1*H*,10*H*-Biindolylidene-2,20-dione (isoindigo) is one of the indigoid natural organic dyes and can be obtained from various natural sources.[23,24] John R. Reynolds research group first used isoindigo (iI) as a new acceptor in iI-based small molecules.[25] The isoindigo-based oligomers showed long wavelength absorption spectra and low HOMO energy levels.[26,27] This group also reported the synthesis of the homopolymer of isoindigo (an acceptor conjugated polymer) and its use in all-polymer BHJ solar cells with P3HT, yielding efficiency approaching 0.5%.[28]

Here, we designed and synthesized two novel conjugated polymers based on EDTT with BDT or isoindigo, respectively, as shown in Scheme 1, and explored their thermal, optical, electrochemical, and photovoltaic properties. In addition, extensive

[a]*Qingdao Institute of Bioenergy and Bioprocess Technology, Chinese Academy of Sciences, Qingdao 266101, P.R. China. E-mail: yangrq@qibebt.ac.cn; Fax: +86-532-80662778; Tel: +86-532-80662700*

[b]*College of Mechanical & Electronic Engineering, Northwest A&F University, Yangling 712100, P.R. China*

† Electronic supplementary information (ESI) available: Synthesis details, device fabrication procedures, current–voltage measurements, FT-IR spectra, XRD spectra, and stability tests. See DOI: 10.1039/c2py20995k

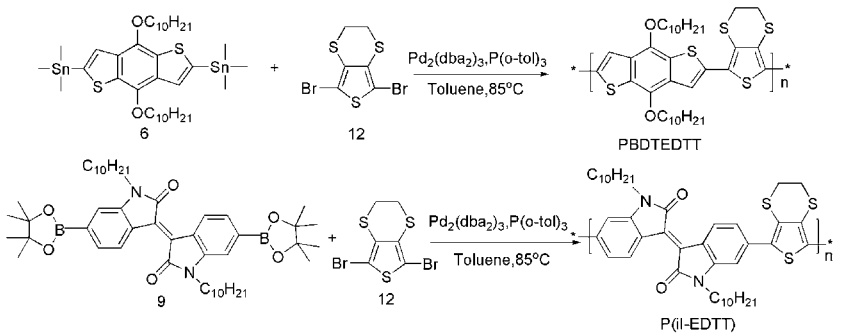

Scheme 1 The synthesis and structures of EDTT-based polymers.

research efforts were focused on improving the performance of the PSCs. Both the conventional cells and inverted cells were fabricated, and solvent additives were used, and the other conditions, such as the ratio of the polymer to $PC_{60}BM$, solvents, concentration, spin-coating speed and annealing temperature, were also carefully optimized. As a result, a PCE of 2.4% was achieved, suggesting that EDTT is a good candidate for the building block applicable to efficient PSCs.

Results and discussion

Design and synthesis of polymers

Based on reports published by other groups, when the copolymer of BDT and thiophene was blended in a bulk heterojunction configuration as the core component for PSC, it exhibited a hole mobility of 0.25 $cm^2\ V^{-1}\ s^{-1}$ which is a quite higher value for conjugated polymers.[29] It is presumed that BDT based polymers can improve mobility due to their large planar conjugated structure. As the all-sulfur analog of EDOT, EDTT exhibits some distinctive properties. For example, EDTT is twisted by 45° compared to EDOT because of the replacement of oxygen atoms by sulfur atoms, which lead to the copolymers becoming less sterically hindered.[30] Accordingly, it is reasonable to presume that copolymers of BDT and EDTT exhibit good mobility. Since the homopolymer of isoindigo is a typical n-type semiconductor,[31] the electron-rich comonomer should be chosen in order to increase the HOMO level of the desired polymers and obtain p-type isoindigo-based polymers.[32] The donor–acceptor interactions of the electron-deficient isoindigo skeleton and electron-rich units enhance the interchain π–π stacking.[33] Therefore, we synthesized two types of copolymers, P(iI-EDTT) and PBDTEDTT. The synthetic routes of the monomers and polymers are illustrated in Scheme S1† and the synthesis and polymerization reactions are provided in detail in the ESI.† PBDTEDTT was synthesized by Stille cross-coupling reactions with a 1 : 1 monomer ratio in the presence of tris(dibenzylideneacetone)-dipalladium ($Pd_2(dba)_3$) as a catalyst and P(*o*-tol)$_3$ as a ligand in dry degassed toluene at 85 °C to give purple-blue materials. P(iI-EDTT) was obtained through the palladium-catalyzed Suzuki coupling method. The crude polymers were purified by silica gel column chromatography using chloroform as the eluent, then precipitated in methanol. The number average molecular weights (M_n) of PBDTEDTT and P(iI-EDTT) were 22 kDa (PDI 2.1) and 19 kDa (PDI 2.3), respectively. The typical FT-IR spectra of PBDTEDTT showed characteristic bands associated with C–O at around 1047 cm^{-1} (Fig. S1†) and the characteristic absorption peak of the C=O stretching in P(iI-EDTT) was exhibited at around 1693 cm^{-1} (Fig. S2†).

Thermal behavior of copolymers was measured using thermogravimetric analysis (TGA) and differential scanning calorimetry (DSC) under a nitrogen atmosphere at atmospheric pressure. TGA indicates that PBDTEDTT and P(iI-EDTT) have good thermal stability with the decomposition temperature (T_d) up to 300 °C (Fig. S3†). The 5% weight loss of PBDTEDTT took place at 331 °C whereas the polymer of P(iI-EDTT) started to degrade at temperatures above 351 °C. DSC reveals that there is no obvious glass transitions for the two polymers (Fig. S4†).

Optical and electrochemical properties

The absorption spectra of the polymers in chloroform solution and in films are shown in Fig. 1, and the data are summarized in Table 1. In dilute chloroform solutions, the absorption peaks of PBDTEDTT and P(iI-EDTT) locate at 494 nm and 612 nm, respectively. In films, the peak of absorption of PBDTEDTT is at about 537 nm, followed by P(iI-EDTT) at 626 nm. The longer

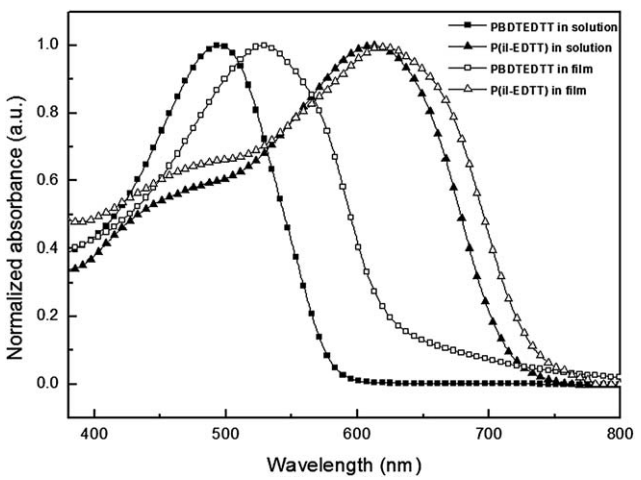

Fig. 1 UV-vis absorption spectra of the polymers in chloroform solution and in films.

Table 1 Optical and electrochemical properties of the copolymers

	Chloroform solution			Thin film			CV		
Polymer	λ_{max} (nm)	λ_{onset} (nm)	E_g^{opt} (eV)	λ_{max} (nm)	λ_{onset} (nm)	E_g^{opt} (eV)	E_{ox}^{ec} (eV)	HOMO (eV)	LUMO (eV)
PBDTEDTT	494	580	2.13	537	637	1.95	0.76	−5.18	−3.23
P(iI-EDTT)	612	714	1.74	626	737	1.68	0.86	−5.28	−3.60

wavelength absorption of P(iI-EDTT) compared to PBDTEDTT is due to a strong D–A charge transfer state, which lead to the extended absorption. The UV-vis absorption spectra of PBDTEDTT and P(iI-EDTT) in films are broader and red-shifted relative to those measured in solution as shown in Fig. 1. This behavior is due to the enhanced intermolecular interactions between the polymer chains and the planarization effect of the π-conjugated polymer backbone, which enable the polymer chains to self-assemble into a well-ordered nanostructure in the solid state. From the different red-shifted wavelengths (43 nm *vs.* 14 nm), one can observe that the planarization effect of PBDTEDTT is stronger than that of P(iI-EDTT) (see XRD spectra in Fig. S9†). The optical bandgaps of PBDTEDTT and P(iI-EDTT) can be estimated at 1.95 and 1.68 eV, respectively, from their onset absorption in the thin film.

Cyclic voltammetry (CV) was performed on a CHI660D electrochemical workstation to determine the redox potentials of the polymers. It is equipped with a three-electrode cell consisting of a glassy carbon working electrode, a saturated calomel reference electrode (SCE) and a platinum wire counter electrode. The measurements were done in anhydrous acetonitrile containing 0.1 M nBu$_4$NPF$_6$ as a supporting electrolyte under an argon atmosphere at a scan rate of 100 mV s^{-1}. Thin films were deposited from chloroform solution onto the working electrodes and dried under nitrogen prior to measurement. The redox potential of the Fc/Fc$^+$ internal reference is 0.38 V *vs.* SCE. The HOMO and LUMO energy levels of the polymers are determined by calculating the empirical formula of $E_{HOMO} = -e(E_{ox} + 4.8 - E_{1/2,(Fc/Fc+)})$, $E_{LUMO} = E_{HOMO} + E_g$, where E_{ox} is estimated from the onset of the oxidation potential and E_g is the solid state optical band gap. The related electrochemical data are summarized in Table 1. The onset oxidation potentials of PBDTEDTT and P(iI-EDTT) are 0.76 V and 0.86 V (Fig. S5†), thus the corresponding HOMO energy levels are −5.18 eV and −5.28 eV, respectively. The deep HOMO energy level of P(iI-EDTT) is desirable for a higher open circuit voltage of the PSCs (Table 2).

Table 2 Device performance of the copolymers

Copolymer	Ratio	Solvent	V_{oc}	J_{sc} (mA cm^{-2})	FF (%)	PCE (%)
PBDTEDTT:PC$_{60}$BM	2.5 : 1	CB	0.69	5.91	51	2.07
PBDTEDTT:PC$_{60}$BM	2 : 1	CB	0.69	6.62	53	2.40
PBDTEDTT:PC$_{60}$BM	1.7 : 1	CB	0.67	5.21	52	1.82
PBDTEDTT:PC$_{60}$BM	1.3 : 1	CB	0.67	3.87	53	1.51
PBDTEDTT:PC$_{60}$BM	1 : 1	CB	0.66	4.21	53	1.47
PBDTEDTT:PC$_{60}$BM	1 : 2	CB	0.60	1.17	33	0.23
P(iI-EDTT):PC$_{60}$BM	1 : 1	1,2-DCB	0.81	1.66	22	0.30

The LUMO energy levels of PBDTEDTT and P(iI-EDTT) are −3.23 eV and −3.60 eV, respectively.

Photovoltaic properties

In order to investigate the potential applications of the two copolymers in solar cells, the bulk heterojunction PSCs were fabricated with a device structure of ITO/PEDOT:PSS/copolymer:PC$_{60}$BM/LiF/Al (Fig. S6†), and tested under a simulated AM 1.5G illumination of 100 mW cm^{-2}. The blends of PBDTEDTT and PC$_{60}$BM at different weight ratios of 2.5 : 1, 2 : 1, 1.7 : 1, 1.3 : 1, 1 : 1 and 1 : 2 were used to optimize the device performance and their current density *versus* voltage (*J–V*) curves are shown in Fig. 2 and S10,† and the detailed device parameters are summarized in Table 2. The other conditions, such as solvents (1,2-dichlorobenzene (DCB) and chlorobenzene (CB)), concentration, spin-coating speed and annealing temperature (Table S1†), were also carefully optimized. Finally, the PCE of 2.4% for the PBDTEDTT polymer was obtained with an open-circuit voltage of 0.69 V, a short circuit current density of 6.62 mA cm^{-2}, and a fill factor of 53%, when the device was made at a donor–acceptor weight ratio of 2 : 1 in CB at a concentration of 10 mg mL^{-1}, spun cast at 1000 rpm and annealed at 120 °C before LiF/Al deposition.

The photoresponse curve of the ITO/PEDOT:PSS (30 nm)/PBDTEDTT:PC$_{60}$BM (100 nm)/LiF (1 nm)/Al (100 nm) device can be seen in Fig. 3. It exhibits a relatively broad photoresponse

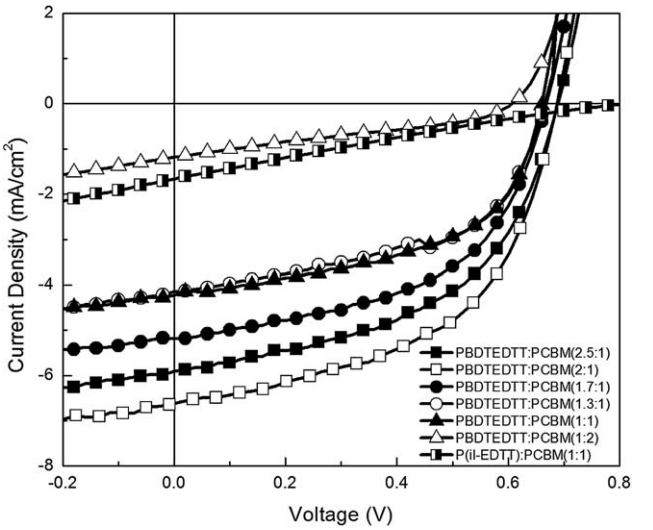

Fig. 2 *J–V* curves of the different ratios of PBDTEDTT:PC$_{60}$BM and P(iI-EDTT):PC$_{60}$BM based BHJ solar cells, under AM 1.5G solar illumination, in conventional architecture.

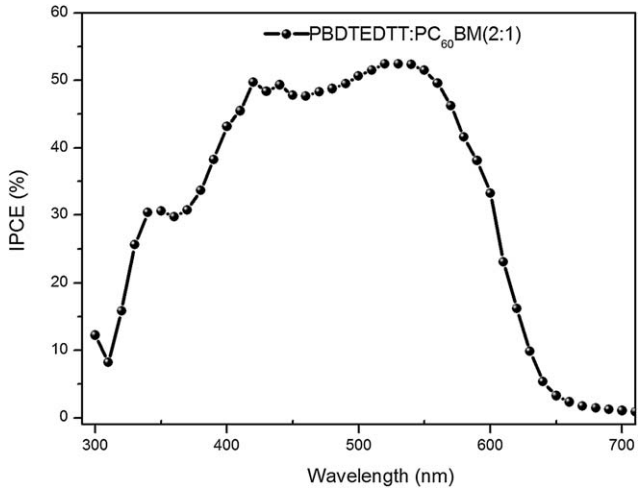

Fig. 3 The incident photon-to-current efficiency (IPCE) of PBDTEDTT:$PC_{60}BM$ with the ratio of 2 : 1 in conventional cells.

range between 300 and 620 nm, indicating that the absorption of the PBDTEDTT:$PC_{60}BM$ blends reflects the photocurrents in these wavelength regions. The device based on PBDTEDTT shows a high maximum incident photon-to-current conversion efficiency (IPCE) value of 53%, which is coincident with the J_{sc} value for the photovoltaic performance of the PBDTEDTT:PCBM PSC device, as mentioned above.

Different ratios of solvent additive 1,8-diiodooctane (DIO) were added, however, no improvement of the performance was observed (Table S2†). The inverted cells based on the structure of ITO/ZnO/PBDTEDTT:$PC_{60}BM$/MoO_3/Ag were also fabricated (Fig. S6†). The PCE of inverted cells was lower compared to those of the conventional ones (Table S2†).

PBDTEDTT demonstrates higher photovoltaic performance over P(iI-EDTT) (Fig. 2 and Table 2), even though P(iI-EDTT) is a D–A copolymer. One potential reason is the poor solubility of P(iI-EDTT) which cannot be dissolved completely in CB and DCB, whereas PBDTEDTT has good solubility in common solvents, such as toluene, chloroform and tetrahydrofuran. Moreover, the atomic force microscopy (AFM) images of PBDTEDTT:$PC_{60}BM$ and P(iI-EDTT):$PC_{60}BM$ blending films are shown in Fig. 4. It is found that the surfaces of PBDTEDTT:$PC_{60}BM$ (2 : 1) composite thin films are very smooth (Fig. 4a), and their root-mean-square (rms) of roughness is about 0.6 nm which indicates the extraordinarily good miscibility between PBDTEDTT and $PC_{60}BM$ in the solid state. The phase images show that the blending film of PBDTEDTT:$PC_{60}BM$ forms interpenetrating structures (Fig. 4b) compared to that of the P(iI-EDTT):$PC_{60}BM$ (1 : 1) blending film (Fig. 4d), which would result in higher charge separation. Therefore, it could improve the photovoltaic performance of the PBDTEDTT:$PC_{60}BM$ blending film. Although the P(iI-EDTT):$PC_{60}BM$ cell has a V_{oc} of 0.81 V which is consistent with the high HOMO energy level of the polymer, the efficiency

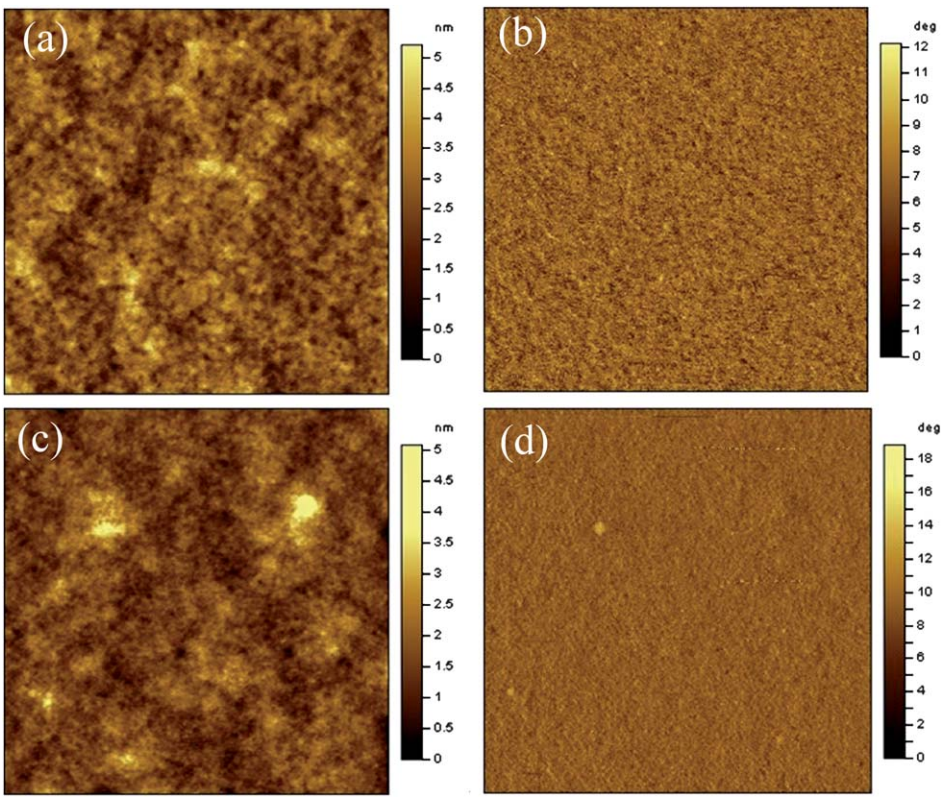

Fig. 4 The AFM tapping mode height (a) and phase (b) images (2 μm × 2 μm) of the PBDTEDTT:$PC_{60}BM$ (2 : 1) film and height (c) and phase (d) images (2 μm × 2 μm) of the P(iI-EDTT):$PC_{60}BM$ (1 : 1) film.

is limited by the low J_{sc} of 1.66 mA cm^{-2} and FF of 22%. This low PCE can be explained by the high surface roughness and very weak phase separation which are observed in the P(iI-EDTT):$PC_{60}BM$ blending film morphology (Fig. 4c and d). This entails a limited donor–acceptor interface in the BHJ, leading to a reduced number of excitons being dissociated in the film.

In order to obtain insight into the nanostructure of the blend films, the cross-sections of the samples were imaged by Scanning Electron Microscopy (SEM). Each layer can be clearly seen from Fig. S7 and S8.† Moreover, the ordering structure of the blend films was investigated using X-ray diffraction (XRD) spectra. As shown in Fig. S9,† the PBDTEDTT:$PC_{60}BM$ (2 : 1) blend film displays a π–π stacking ($2\theta = 27.7°$) peak whereas only the peak corresponding to the ITO substrate ($2\theta = 21.6°$) can be detected in the P(iI-EDTT):$PC_{60}BM$ (1 : 1) blend film, which could be another potential reason that PBDTEDTT exhibits better performance compared to P(iI-EDTT) with a less ordered structure.

The stability of the devices was also evaluated using a conventional cell architecture. The results can be seen from Fig. S11–14.† When these devices were well encapsulated, they showed a good stability.

Conclusion

In summary, two novel copolymers, PBDTEDTT and P(iI-EDTT), were synthesized, in which 3,4-ethylenedithiathiophene was incorporated into the backbone. The absorption spectra of the P(iI-EDTT) polymer ranges from 400 nm to 737 nm, almost covering the whole visible region. The maximum PCE of 2.4% for PBDTEDTT was obtained with an open-circuit voltage of 0.69 V, a short circuit current of 6.62 mA cm^{-2}, and a fill factor of 53%. However, the device based on P(iI-EDTT):$PC_{60}BM$ had much lower J_{sc}, FF and PCE, although it had higher V_{oc}. It could be explained by the molecular structure, π–π stacking, solubility and morphology of the film. Our preliminary results exhibited that EDTT is a promising donor unit, and when it is combined with a suitable building block, the resultant polymer would give high photovoltaic performance.

Acknowledgements

This work was supported by the Ministry of Science and Technology of China (2010DFA52310), National Natural Science Foundation of China (21204097, 51173199, 61107090), Chinese Academy of Sciences ("One Hundred Talented Program", and KGCX2-YW-399+9-2), Department of Science and Technology of Shandong Province (2010GGC10345), Shandong Provincial Natural Science Foundation (ZR2011BZ007), and Qingdao Municipal Science and Technology Program (11-2-4-22-hz).

Notes and references

1 G. Yu, J. Gao, J. C. Hummelen, F. Wudl and A. J. Heeger, *Science*, 1995, **270**, 1789–1791.
2 J. Huo, L. Wang, E. Irran, H. Yu, J. Gao, D. Fan, B. Li, J. Wang, W. Ding, A. M. Amin, C. Li and L. Ma, *Angew. Chem., Int. Ed.*, 2010, **49**, 9237–9241.
3 J. C. Bijleveld, A. P. Zoombelt, S. G. J. Mathijssen, M. M. Wienk, M. Turbiez, D. M. de Leeuw and R. A. J. Janssen, *J. Am. Chem. Soc.*, 2009, **131**, 16616–16617.
4 H. Zhou, L. Yang and W. You, *Macromolecules*, 2012, **45**, 607–632.
5 T. M. Clarke and J. R. Durrant, *Chem. Rev.*, 2010, **110**, 6736–6767.
6 N. S. Lewis, *Science*, 2007, **315**, 798–801.
7 R. C. Coffin, J. Peet, J. Rogers and G. C. Bazan, *Nat. Chem.*, 2009, **1**, 657–661.
8 Y.-J. Cheng, S.-H. Yang and C.-S. Hsu, *Chem. Rev.*, 2009, **109**, 5868–5923.
9 O. InganÄs, F. Zhang and M. R. Andersson, *Acc. Chem. Res.*, 2009, **42**, 1731–1739.
10 Y. Li and Y. Zou, *Adv. Mater.*, 2008, **20**, 2952–2958.
11 Z. He, C. Zhong, X. Huang, W.-Y. Wong, H. Wu, L. Chen, S. Su and Y. Cao, *Adv. Mater.*, 2011, **23**, 4636–4643.
12 Y. Li, *Acc. Chem. Res.*, 2012, **45**, 723–733.
13 I. Winter, C. Reese, J. Hormes, G. Heywang and F. Jonas, *Chem. Phys.*, 1995, **194**, 207–213.
14 Y. H. Wijsboom, Y. Sheynin, A. Patra, N. Zamoshchik, R. Vardimon, G. Leitus and M. Bendikov, *J. Mater. Chem.*, 2011, **21**, 1368–1372; E. Poverenov, Y. Sheynin, N. Zamoshchik, A. Patra, G. Leitus, I. F. Perepichka and M. Bendikov, *J. Mater. Chem.*, 2012, **22**, 14645–14655.
15 Z. Xu, J.-H. Kang, F. Wang, S.-M. Paek, S.-J. Hwang, Y. Kim, S.-J. Kim, J.-H. Choy and J. Yoon, *Tetrahedron Lett.*, 2011, **52**, 2823–2825.
16 H. J. Spencer, R. Berridge, D. J. Crouch, S. P. Wright, M. Giles, I. McCulloch, S. J. Coles, M. B. Hursthouse and P. J. Skabara, *J. Mater. Chem.*, 2003, **13**, 2075–2077.
17 H. Pang, P. J. Skabara, S. Gordeyev, J. J. W. McDouall, S. J. Coles and M. B. Hursthouse, *Chem. Mater.*, 2006, **19**, 301–307.
18 O. Fadhel, Z. Benkö, M. Gras, V. Deborde, D. Joly, C. Lescop, L. Nyulászi, M. Hissler and R. Réau, *Chem.–Eur. J.*, 2010, **16**, 11340–11356.
19 S. Chen, B. Lu, X. Duan and J. Xu, *J. Polym. Sci., Part A: Polym. Chem.*, 2012, **50**, 1967–1978.
20 C. Piliego, T. W. Holcombe, J. D. Douglas, C. H. Woo, P. M. Beaujuge and J. M. J. Fréchet, *J. Am. Chem. Soc.*, 2010, **132**, 7595–7597.
21 W. Chen, T. Xu, F. He, W. Wang, C. Wang, J. Strzalka, Y. Liu, J. Wen, D. J. Miller, J. Chen, K. Hong, L. Yu and S. B. Darling, *Nano Lett.*, 2011, **11**, 3707–3713.
22 J. H. Hou, M. H. Park, S. Q. Zhang, Y. Yao, L. M. Chen, J. H. Li and Y. Yang, *Macromolecules*, 2008, **41**, 6012–6018.
23 S. Albrecht, S. Janietz, W. Schindler, J. Frisch, J. Kurpiers, J. Kniepert, S. Inal, P. Pingel, K. Fostiropoulos, N. Koch and D. Neher, *J. Am. Chem. Soc.*, 2012, **134**, 14932–14944.
24 L. A. Estrada, D. Y. Liu, D. H. Salazar, A. L. Dyer and J. R. Reynolds, *Macromolecules*, 2012, **45**, 8211–8220.
25 J. Mei, K. R. Graham, R. Stalder and J. R. Reynolds, *Org. Lett.*, 2010, **12**, 660–663.

26 E. Wang, Z. Ma, Z. Zhang, K. Vandewal, P. Henriksson, O. Inganäs, F. Zhang and M. R. Andersson, *J. Am. Chem. Soc.*, 2011, **133**, 14244–14247.
27 T. Lei, Y. Cao, Y. Fan, C.-J. Liu, S.-C. Yuan and J. Pei, *J. Am. Chem. Soc.*, 2011, **133**, 6099–6101.
28 R. Stalder, J. Mei, J. Subbiah, C. Grand, L. A. Estrada, F. So and J. R. Reynolds, *Macromolecules*, 2011, **44**, 6303–6310.
29 H. Pan, Y. Li, Y. Wu, P. Liu, B. S. Ong, S. Zhu and G. Xu, *J. Am. Chem. Soc.*, 2007, **129**, 4112–4113.
30 M. Turbiez, P. Frère, M. Allain, N. Gallego-Planas and J. Roncali, *Macromolecules*, 2005, **38**, 6806–6812.
31 E. Wang, Z. Ma, Z. Zhang, P. Henriksson, O. Inganas, F. Zhang and M. R. Andersson, *Chem. Commun.*, 2011, **47**, 4908–4910.
32 W. Ying, F. Guo, J. Li, Q. Zhang, W. Wu, H. Tian and J. Hua, *ACS Appl. Mater. Interfaces*, 2012, **4**, 4215–4224.
33 G. Zhang, Y. Fu, Z. Xie and Q. Zhang, *Macromolecules*, 2011, **44**, 1414–1420.

